COMPARISON OF METHODS IN CALCULATING FREQUENCIES OF CORNER-SUPPORTED RECTANGULAR PLATES

by Robert E. Reed, Jr.

Ames Research Center

Moffett Field, Calif.
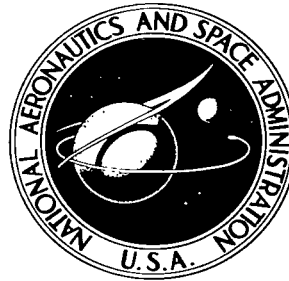
NASA TN D-3030

COMPARISON OF METHODS IN CALCULATING FREQUENCIES OF

CORNER-SUPPORTED RECTANGULAR PLATES

By Robert E. Reed, Jr.

Ames Research Center
Moffett Field, Calif.

NATIONAL AERONAUTICS AND SPACE ADMINISTRATION

COMPARISON OF METHODS IN CALCULATING FREQUENCIES OF

CORNER-SUPPORTED RECTANGULAR PLATES

By Robert E. Reed, Jr.
Ames Research Center

SUMMARY

The lower natural frequencies of a rectangular plate that is pin supported at the corners are found analytically by two approximate methods. The first is the Ritz method and the second is a series solution to the differential equation of motion. These frequencies are also found experimentally for comparison. All of the results are presented along with some previous work done by other authors using a finite difference method. Some of the advantages and disadvantages of the two methods pertaining to the numerical computations are discussed.

INTRODUCTION

The linear equation of motion, based on the Kirchoff plate theory, for the free transverse vibration of thin rectangular plates is well known but exact solutions have been found for just a few types of boundary conditions. For more difficult cases, approximate methods are available for calculating the natural frequencies and mode shapes and have been extensively applied by various authors to problems in which the plate is supported along entire boundaries (see, e.g., ref. 1, ch. 7). In the following, two approximate methods, which can be applied to many other problems, are used for determining the natural frequencies and mode shapes of a rectangular plate with isolated pin supports at the corners. This problem is of interest since it is common design practice to support panels at isolated points (e.g., solar panels, hatches, covers, etc.) and also because the solutions point out some of the difficulties that can be encountered in plate vibration problems when approximate methods are used.

The first method used is the well-known Ritz method. Natural frequencies and mode shapes of the lower modes were calculated to what appeared to be about 1-percent accuracy by using more and more terms of the assumed series until the result indicated (at least to the author) the convergence to the desired accuracy. However, some of the numerical examples calculated herein were previously treated by Cox and Boxer (ref. 2) who used the approximate method of solving the finite difference equations of motion on a digital computer. Upon comparison with their work (they felt their answers were accurate to within about 1 percent), discrepancies in natural frequency were found to be as large as 10 percent. Instead of exploring the convergence of the Ritz method, a series solution to the differential equation of motion was obtained and the calculated frequencies showed that, in most cases, the discrepancies

were due to the slow convergence of the Ritz method. A short experimental program was then undertaken to see the correlation between experiment and theory. All of the results are presented herein for comparison along with a discussion of the problems associated with the methods and their adaptation to the computer.

NOTATION

A_{ni} integration constants, i = 1, 2, 3, 4

a   length of plate

B_{ni} integration constants, i = 1, 2, 3, 4

b   width of plate

D   bending rigidity of plate, $\dfrac{Eh^3}{12(1 - \nu^2)}$

E   Young's modulus

g   acceleration of gravity

h   plate thickness

i,j,k,l,m,n   summation indices

L_0 $\dfrac{a}{b}$

T_{max} amplitude of kinetic energy

t   time

V_{max} amplitude of strain energy

$W(x,y,t)$ transverse displacement

$w(x,y)$ amplitude of $W(x,y,t)$

x,y   Cartesian coordinates

α_n $\dfrac{n\pi}{a}$

β_n $\dfrac{n\pi}{b}$

γ weight density

λ dimensionless frequency parameter, $\dfrac{\omega a^2}{\pi^2}\sqrt{\dfrac{\gamma h}{Dg}}$

ν Poisson's ratio

ω circular frequency

METHODS OF ANALYZING PLATES ON ISOLATED SUPPORTS

The form of an approximate solution for a plate on isolated supports can sometimes be obtained from the solution for the more common problem of a plate supported along entire edges. For a rectangular plate, this latter solution can usually be chosen as

$$w = \sum_m \sum_n a_{mn} F_m(x) G_n(y)$$

where the displacement $W(x,y,t) = w(x,y)\sin \omega t$ and the function $F_m(x)G_n(y)$ and its derivatives can satisfy certain conditions along the lines $x = $ constant and $y = $ constant but cannot satisfy restraint conditions at isolated points. For a plate on isolated supports, a superposition of solutions of this type can be used so that each part satisfies conditions along certain, but different, lines and the intersection of these lines are at the isolated supports. For example, the sketch below shows a plate on three supports. Let w be of the form

$$w = \sum_m \sum_n \left[a_{mn} F_m^{(1)}(x) G_n^{(1)}(y) + b_{mn} F_m^{(2)}(x) G_n^{(2)}(y) \right]$$
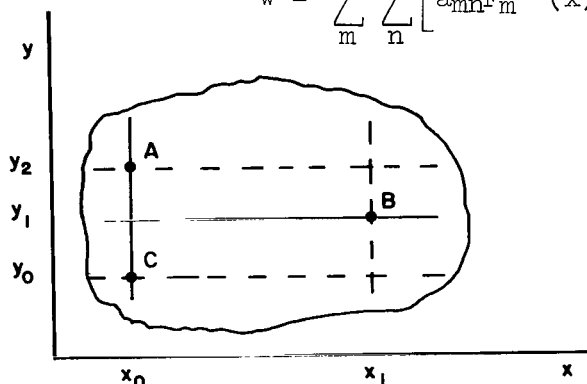
Example of plate on three supports

where $F_m^{(1)}(x)G_n^{(1)}(y)$ satisfy zero displacement conditions along the lines $x = x_0$, $y = y_1$. The functions $F_m^{(2)}(x)G_n^{(2)}(y)$ satisfy zero displacement along the lines $y = y_0$, $y = y_2$, and $x = x_1$. The functions $a_{mn} F_m^{(1)}(x) G_n^{(1)}(y) + b_{mn} F_m^{(2)}(x) G_n^{(2)}(y)$ then have zero displacements at just the points A, B, and C.
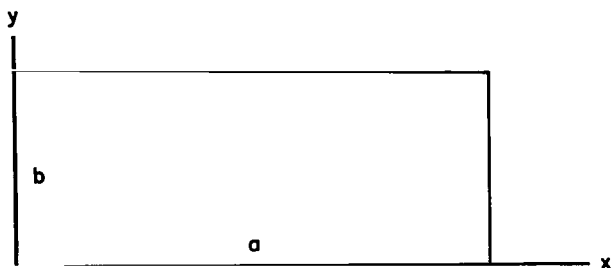
Corner-supported rectangular plate

Corner-Supported Rectangular Plates

The plate being considered in the present report is shown in the adjacent sketch. The solution can be taken as

$$w(x,y) = w_1(x,y) + w_2(x,y)$$

where

$$w_1(0,y) = w_1(a,y) = 0$$

$$w_2(x,0) = w_2(x,b) = 0$$

3

The complete boundary conditions are:

<u>Displacements</u>:

$$w(0,0) = w(0,b) = w(a,0) = w(a,b) = 0$$

<u>Moments</u>:

$$\frac{\partial^2 w}{\partial x^2}(0,y) + \nu \frac{\partial^2 w}{\partial y^2}(0,y) = 0 \qquad\qquad \frac{\partial^2 w}{\partial x^2}(a,y) + \nu \frac{\partial^2 w}{\partial y^2}(a,y) = 0$$

$$\frac{\partial^2 w}{\partial y^2}(x,0) + \nu \frac{\partial^2 w}{\partial x^2}(x,0) = 0 \qquad\qquad \frac{\partial^2 w}{\partial y^2}(x,b) + \nu \frac{\partial^2 w}{\partial x^2}(x,b) = 0$$

<u>Effective shear forces</u>:

$$\frac{\partial^3 w}{\partial x^3}(0,y) + (2-\nu)\frac{\partial^3 w}{\partial x\, \partial y^2}(0,y) = 0 \qquad \frac{\partial^3 w}{\partial x^3}(a,y) + (2-\nu)\frac{\partial^3 w}{\partial x\, \partial y^2}(a,y) = 0$$

$$\frac{\partial^3 w}{\partial y^3}(x,0) + (2-\nu)\frac{\partial^3 w}{\partial x^2\, \partial y}(x,0) = 0 \qquad \frac{\partial^3 w}{\partial y^3}(x,b) + (2-\nu)\frac{\partial^3 w}{\partial x^2\, \partial y}(x,b) = 0$$

The reactions at the corners are given by $2M_{xy}$ evaluated at the corners (this is the corner force that arises when the shear Q_x or Q_y is combined with the rate of change of the twisting moment M_{xy} to give the effective shear V_x or V_y)(ref. 3).

<u>Ritz method solution</u>.- The Ritz method is well known (ref. 4) and is based on the fact that for a freely vibrating system, for which the motion is harmonic, the sum of potential and kinetic energy is a constant and the maximum values (with respect to time) of these forms of energy are equal to each other. If the time dependent displacement is denoted by $W(x,y,t)$, it can be written in the form

$$W(x,y,t) = w(x,y)\sin \omega t$$

If $w(x,y)$ is of the form

$$w(x,y) = \sum_m \sum_n \left[a_{mn}F_m^{(1)}(x)G_n^{(1)}(y) + b_{mn}F_m^{(2)}(x)G_n^{(2)}(y) \right] \qquad (1)$$

4

the ratios of the unknown a's and b's and the natural frequencies can be determined from the set of linear algebraic equations obtained from

$$\frac{\partial}{\partial a_{ij}} \left(V_{max} - T_{max}\right) = 0 \left.\begin{array}{c} \\ \\ \\ \\ \\ \end{array}\right\} \quad (2)$$

$$\frac{\partial}{\partial b_{ij}} \left(V_{max} - T_{max}\right) = 0 \qquad i,j = 1,2,\ldots$$

where, in this case,

$$V_{max} = \frac{D}{2} \int_{o}^{b} \int_{o}^{a} \left[\left(\frac{\partial^2 w}{\partial x^2}\right)^2 + \left(\frac{\partial^2 w}{\partial y^2}\right)^2 + 2\nu \frac{\partial^2 w}{\partial x^2} \frac{\partial^2 w}{\partial y^2} + 2(1-\nu)\left(\frac{\partial^2 w}{\partial x \partial y}\right)^2\right] dx\, dy \qquad (3)$$

$$T_{max} = \frac{\omega^2 \gamma h}{2g} \int_{o}^{b} \int_{o}^{a} w^2\, dx\, dy \qquad (4)$$

Each term of the series in equation (1) must satisfy the boundary conditions on the displacements and rotations but does not have to satisfy those on stress (ref. 4). Of course, one would expect that fewer terms of equation (1) would be needed to represent a mode if some or all of the stress boundary conditions were satisfied. Also, it is known that the frequency calculated for a particular mode from an approximate form of w will be above the exact answer (ref. 4).

For the problem being considered, the displacement is chosen to be

$$w = \sum_{n=1}\left(a_{on} \sin\frac{n\pi y}{b} + b_{on} \sin\frac{n\pi x}{a}\right) + \sum_{m=1}\sum_{n=1}\left(a_{mn} \cos\frac{m\pi x}{a} \sin\frac{n\pi y}{b}\right.$$

$$\left. + b_{mn} \cos\frac{m\pi y}{b} \sin\frac{n\pi x}{a}\right) \qquad (5)$$

where the single summation contains the m = 0 terms of the double summation. One should note that for each value of m and n, equation (5) satisfies the displacement boundary conditions but does not satisfy either the moment or transverse shear boundary condition. Equations (2) will be of the form

$$\frac{\partial V_{max}}{\partial a_{oj}} - \frac{\partial T_{max}}{\partial a_{oj}} = 0 \qquad (6)$$

5

$$\frac{\partial V_{max}}{\partial a_{ij}} - \frac{\partial T_{max}}{\partial a_{ij}} = 0 \tag{7}$$

$$\frac{\partial V_{max}}{\partial b_{oj}} - \frac{\partial T_{max}}{\partial b_{oj}} = 0 \tag{8}$$

$$\frac{\partial V_{max}}{\partial b_{ij}} - \frac{\partial T_{max}}{\partial b_{ij}} = 0 \qquad \begin{aligned} i &= 1,2,3,\ldots \\ j &= 1,2,3,\ldots \end{aligned} \tag{9}$$

Substitution of equation (5) and its derivatives into equations (3) and (4) and integrating over the surface of the plate will give V_{max} and T_{max} in terms of the a_{ij}'s and b_{ij}'s. Then, substitution of V_{max} and T_{max} into equations (6) through (9) will give the following algebraic equations from which the frequency parameter λ^2, where $\lambda^2 = (a^4/\pi^4)(\gamma h \omega^2/Dg)$ and $L_o = a/b$, can be determined:

$$a_{oj}2(j^4L_o^4 - \lambda^2) + \frac{4[(-1)^j-1]}{\pi^2 j} \sum_{n=1} \frac{b_{on}}{n} [(-1)^n-1](\nu n^2 j^2 L_o^2 - \lambda^2)$$

$$+ \frac{4j}{\pi^2} \sum_{\substack{m,n=1 \\ m \neq j}} \frac{b_{mn}}{n(j^2-m^2)} [(-1)^n-1][(-1)^j(-1)^m-1](m^2 j^2 L_o^4 + \nu n^2 j^2 L_o^2 - \lambda^2) = 0 \tag{10}$$

$$b_{oj}2(j^4 - \lambda^2) + \frac{4[(-1)^j-1]}{\pi^2 j} \sum_{n=1} \frac{a_{on}}{n} [(-1)^n-1](\nu n^2 j^2 L_o^2 - \lambda^2)$$

$$+ \frac{4j}{\pi^2} \sum_{\substack{m,n=1 \\ m \neq j}} \frac{a_{mn}}{n(j^2-m^2)} [(-1)^n-1][(-1)^j(-1)^m-1](m^2 j^2 + \nu n^2 j^2 L_o^2 - \lambda^2) = 0 \tag{11}$$

$$a_{ij}[(i^2 + j^2 L_o^2)^2 - \lambda^2] + \frac{4[(-1)^j-1]}{\pi^2 j} \sum_{\substack{n=1 \\ n \neq i}} \frac{b_{on} n}{n^2-i^2} [(-1)^n(-1)^i-1](n^2 i^2 + \nu n^2 j^2 L_o^2 - \lambda^2)$$

$$+ \frac{4j}{\pi^2} \sum_{\substack{m,n=1 \\ m \neq j, n \neq i}} b_{mn} n \frac{[(-1)^i(-1)^n-1][(-1)^j(-1)^m-1]}{(n^2-i^2)(j^2-m^2)} [n^2 i^2 + m^2 j^2 L_o^4 + (2-\nu)m^2 i^2 L_o^2 + \nu n^2 j^2 L_o^2 - \lambda^2] = 0 \tag{12}$$

$$b_{ij}[(i^2 L_o^2 + j^2)^2 - \lambda^2] + \frac{4[(-1)^j-1]}{\pi^2 j} \sum_{\substack{n=1 \\ n \neq i}} \frac{a_{on} n}{n^2-i^2} [(-1)^n(-1)^i-1](n^2 i^2 L_o^4 + \nu n^2 j^2 L_o^2 - \lambda^2)$$

$$+ \frac{4j}{\pi^2} \sum_{\substack{m,n=1 \\ m \neq j, n \neq i}} \frac{a_{mn} n[(-1)^m(-1)^j-1][(-1)^n(-1)^i-1]}{(n^2-i^2)(j^2-m^2)} [m^2 j^2 + n^2 i^2 L_o^4 + (2-\nu)m^2 i^2 L_o^2 + \nu n^2 j^2 L_o^2 - \lambda^2] = 0 \tag{13}$$

6

In equations (10) through (13), each value of i and j gives a single equation and m and n are dummy indices. The summation notation is

$$\sum_{\substack{m,n=1 \\ m\neq j, n\neq i}} = \sum_{\substack{m=1 \\ m\neq j}} \sum_{\substack{n=1 \\ n\neq i}} (\ldots)$$

Inspection of these equations shows that they uncouple into four groups of equations. Each of these groups represents modes containing a certain type of symmetry or antisymmetry as follows:

(1) a_{ij}; i = even, j = odd

   b_{mn}; m = even, n = odd

   a_{01}, a_{03}, a_{21}, $\ldots$ b_{01}, b_{03}, b_{21}, $\ldots$

$\left. \vphantom{\begin{matrix} a \\ b \\ c \end{matrix}} \right\}$ modes symmetric about the lines $x = \dfrac{a}{2}$ and $y = \dfrac{b}{2}$

(2) a_{ij}; i = odd, j = odd

   b_{mn}; m = even, n = even

   a_{11}, a_{13}, a_{31}, $\ldots$ b_{02}, b_{04}, b_{24}, $\ldots$

$\left. \vphantom{\begin{matrix} a \\ b \\ c \end{matrix}} \right\}$ modes symmetric about $y = \dfrac{b}{2}$ and antisymmetric about $x = \dfrac{a}{2}$

(3) a_{ij}; i = even, j = even

   b_{mn}; m = odd, n = odd

   a_{02}, a_{04}, a_{24}, $\ldots$ b_{11}, b_{13}, b_{31}, $\ldots$

$\left. \vphantom{\begin{matrix} a \\ b \\ c \end{matrix}} \right\}$ modes symmetric about $x = \dfrac{a}{2}$ and antisymmetric about $y = \dfrac{b}{2}$

(4) a_{ij}; i = odd, j = even

   b_{mn}; m = odd, n = even

   a_{12}, a_{14}, a_{32}, $\ldots$ b_{12}, b_{14}, b_{32}, $\ldots$

$\left. \vphantom{\begin{matrix} a \\ b \\ c \end{matrix}} \right\}$ modes antisymmetric about the lines $x = \dfrac{a}{2}$ and $y = \dfrac{b}{2}$

Combinations (2) and (3) are equal for a square plate and are related to each other by the ratio L_0 for rectangular plates. These four combinations of equations are given in appendix A. The equations of each combination can be treated separately and will have the matrix form

$$\begin{bmatrix} & & 0 & & & \\ & A & & & C & \\ 0 & & & & & 0 \\ \hline & & & & & \\ & C & & B & & \\ & & 0 & & & \end{bmatrix} \left\{ \begin{matrix} a_{ij} \\ \vdots \\ a_{k\ell} \\ \overline{b_{mn}} \\ \vdots \\ b_{pq} \end{matrix} \right\} = \left\{ 0 \right\}$$

where the matrix is symmetric and all of the elements of the C array are nonzero. Each nonzero element of the matrix is of the form $k_{ij}-\lambda^2 l_{ij}$. Although these equations are not in the standard eigenvalue form of

$$\left[[A] - \lambda^2 \left[\diagdown I \diagdown \right]\right]\{D\} = 0$$

the roots of the determinant of the coefficient matrix and the mode shapes can be found with existing subroutines.

   Trigonometric series solution.- An appropriate solution to the differential equation of motion can be found in the form of an infinite series. The differential equation is

$$\frac{\partial^4 w}{\partial x^4} + 2 \frac{\partial^4 w}{\partial x^2 \partial y^2} + \frac{\partial^4 w}{\partial y^4} - \zeta^4 w = 0 \tag{14}$$

where

$$\zeta^4 = \frac{\gamma h \omega^2}{Dg} \tag{15}$$

Using the same method discussed earlier, one finds an appropriate form of w which satisfies the displacement boundary conditions as being

$$w = \sum_{n=1}^{\infty} f_n(y) \sin \frac{n\pi x}{a} + \sum_{n=1}^{\infty} g_n(x) \sin \frac{n\pi y}{b} \tag{16}$$

Upon separation of variables, the unknown functions must satisfy the following equations:

$$\frac{d^4 f_n(y)}{dy^4} - 2\alpha_n^2 \frac{d^2 f_n(y)}{dy^2} + (\alpha_n^4 - \zeta^4) f_n(y) = 0 \tag{17}$$

$$\frac{d^4 g_n(x)}{dx^4} - 2\beta_n^2 \frac{d^2 g_n(x)}{dx^2} + (\beta_n^4 - \zeta^4) g_n(x) = 0 \tag{18}$$

where $\alpha_n = n\pi/a$, $\beta_n = n\pi/b$; and $f_n(y)\sin(n\pi x/a)$ is assumed to be linearly independent of $g_n(x)\sin(n\pi y/b)$. Some confusion can result if they are not independent, that is, $f_n(y) = A \sin(n\pi y/b)$ and $g_n(x) = B \sin(n\pi x/a)$. Appendix B discusses this problem.

   Since the coefficients of equations (17) and (18) are constant, the solutions are easily found to be

$$f_n(y) = A_{n1} \cosh \theta_n y + A_{n2} \sinh \theta_n y + A_{n3} \cos \overline{\theta}_n y + A_{n4} \sin \overline{\theta}_n y \tag{19}$$

$$g_n(x) = B_{n1} \cosh \varphi_n x + B_{n2} \sinh \varphi_n x + B_{n3} \cos \overline{\varphi}_n x + B_{n4} \sin \overline{\varphi}_n x \tag{20}$$

8

where

$$\left.\begin{array}{ll} \theta_n = \sqrt{\zeta^2 + \alpha_n^2} & \overline{\theta}_n = \sqrt{\zeta^2 - \alpha_n^2} \\[2ex] \varphi_n = \sqrt{\zeta^2 + \beta_n^2} & \overline{\varphi}_n = \sqrt{\zeta^2 - \beta_n^2} \end{array}\right\} \quad (21)$$

It should be pointed out that $\overline{\theta}_n, \overline{\varphi}_n$ can be real or imaginary, depending on the relative value of λ and α_n or β_n. If $\overline{\theta}_n$ or $\overline{\varphi}_n$ is imaginary, then the trigonometric function in equations (19) or (20) becomes the corresponding hyperbolic function.

Referring to the boundary conditions given by equation (3), equation (16) is seen to identically satisfy the zero displacement conditions at the corners. The conditions for zero bending moment give the following:

$$\left.\begin{array}{l} \dfrac{d^2 g_n(0)}{dx^2} - \nu\beta_n^2 g_n(0) = 0 \\[3ex] \dfrac{d^2 g_n(a)}{dx^2} - \nu\beta_n^2 g_n(a) = 0 \\[3ex] \dfrac{d^2 f_n(0)}{dy^2} - \nu\alpha_n^2 f_n(0) = 0 \\[3ex] \dfrac{d^2 f_n(b)}{dy^2} - \nu\alpha_n^2 f_n(b) = 0 \end{array}\right\} \quad (22)$$

The condition of the effective shear being zero gives the following equations:

$$\left.\begin{array}{l} \displaystyle\sum_{n=1}^{\infty} \alpha_n \left[(2-\nu)\dfrac{d^2 f_n(y)}{dy^2} - \alpha_n^2 f_n(y)\right] + \sum_{n=1}^{\infty}\left[\dfrac{d^3 g_n(0)}{dx^3} - (2-\nu)\beta_n^2 \dfrac{dg_n(0)}{dx}\right]\sin\beta_n y = 0 \\[3ex] \displaystyle\sum_{n=1}^{\infty} \alpha_n(-1)^n \left[(2-\nu)\dfrac{d^2 f_n(y)}{dy^2} - \alpha_n^2 f_n(y)\right] + \sum_{n=1}^{\infty}\left[\dfrac{d^3 g_n(a)}{dx^3} - (2-\nu)\beta_n^2 \dfrac{dg_n(a)}{dx}\right]\sin\beta_n y = 0 \\[3ex] \displaystyle\sum_{n=1}^{\infty} \beta_n \left[(2-\nu)\dfrac{d^2 g_n(x)}{dx^2} - \beta_n^2 g_n(x)\right] + \sum_{n=1}^{\infty}\left[\dfrac{d^3 f_n(0)}{dy^3} - (2-\nu)\alpha_n^2 \dfrac{df_n(0)}{dy}\right]\sin\alpha_n x = 0 \\[3ex] \displaystyle\sum_{n=1}^{\infty} \beta_n(-1)^n \left[(2-\nu)\dfrac{d^2 g_n(x)}{dx^2} - \beta_n^2 g_n(x)\right] + \sum_{n=1}^{\infty}\left[\dfrac{d^3 f_n(b)}{dy^3} - (2-\nu)\alpha_n^2 \dfrac{df_n(b)}{dy}\right]\sin\alpha_n x = 0 \end{array}\right\} \quad (23)$$

For the bending moment, equations (22) show that the constants can be determined so that each term of the series in equation (16) identically satisfies the condition of zero moment on the edge. Equations (23) show that the effective shear boundary condition is satisfied only by a sum of terms. Equations (23) can be simplified by multiplying by the appropriate orthogonal trigonometric function and by integrating over the plate interval. For example, the first one of equations (23) becomes

$$\sum_{n=1} \alpha_n \int_o^b \left[(2-\nu) \frac{d^2 f_n(y)}{dy^2} - \alpha_n{}^2 f_n(y) \right] \sin \beta_m y \, dy$$

$$+ \frac{b}{2} \left[\frac{d^3 g_m(0)}{dx^3} - (2-\nu)\beta_m{}^2 \frac{dg_m(0)}{dx} \right] = 0$$

$$\vdots \tag{24}$$

The integrals in equation (24) can be evaluated and the resulting four sets of equations are in terms of the eight sets of unknown constants, $A_{n1}, \ldots, A_{n4}$, $B_{n1}, \ldots, B_{n4}$. For the integrated equations it is assumed that $\bar{\theta}_n \neq \beta_m$. The condition that $\bar{\theta}_n \neq \beta_m$ is connected with the assumption that $f_n(y) \sin \alpha_n x$ is independent of $g_m(x) \sin \beta_m y$ and is discussed in appendix B.

Four of the eight sets of constants can easily be eliminated from equation (24) by use of equations (22). This results in having a set of 4N simultaneous homogeneous algebraic equations to solve (after truncating the infinite series at $n = N$ terms). These equations are given here because they can easily be programmed for a digital computer, and additional modes and frequencies, to those given herein, can be calculated. (See the Numerical Computations section for a discussion of some of the numerical problems and ways to, at least partially, avoid them.) In these equations, the following notation is used:

$$\left. \begin{array}{l} \lambda^2 = \zeta^4 \dfrac{a^4}{\pi^4} = \dfrac{a^4 \gamma h \omega^2}{\pi^4 D g} \\[2ex] \bar{\theta}_n{}^* = \dfrac{\pi}{L_o} \sqrt{\lambda - n^2} \ , \qquad \theta_n{}^* = \dfrac{\pi}{L_o} \sqrt{\lambda + n^2} \\[2ex] \bar{\varphi}_n{}^* = \pi \sqrt{\lambda - n^2 L_o{}^2} \ , \qquad \varphi_n{}^* = \pi \sqrt{\lambda + n^2 L_o{}^2} \end{array} \right\} \tag{25}$$

$$P_1(\xi,\rho) = \frac{2[(2-\nu)\lambda^3 + (1-\nu)^2 \xi^2 \beta^2 \lambda]}{[-\lambda^2 + (\xi^2 + \rho^2)^2][\lambda + (1-\nu)\xi^2]} \tag{26}$$

$$P_2(\xi) = \frac{\sqrt{\lambda + \xi^2} \ [\lambda - (1-\nu)\xi^2]^2}{[\lambda + (1-\nu)\xi^2]} \tag{27}$$

$$P_3(\xi) = \sqrt{\lambda - \xi^2}\ [\lambda + (1-\nu)\xi^2] \tag{28}$$

where ξ, ρ are used here as dummy variables. The equations are

$$\sum_{n=1}^{N} n(-1)^n P_1(n, mL_0)\{-A_{n3}[1 - (-1)^m \cos \overline{\theta}^*] + (-1)^m A_{n4} \sin \overline{\theta}_n^*\}$$

$$+ \frac{\pi}{2mL_0{}^2} \left\{ B_{m3} \left[P_2(mL_0)\ \frac{\cos \overline{\varphi}_m^* \cosh \varphi_m^* - 1}{\sinh \varphi_m^*} + P_3(mL_0) \sin \overline{\varphi}_m^* \right] \right.$$

$$\left. + B_{m4} \left[P_2(mL_0)\ \frac{\cosh \varphi_m^* \sin \overline{\varphi}_m^*}{\sinh \varphi_m^*} - P_3(mL_0) \cos \overline{\varphi}_m^* \right] \right\} = 0 \tag{29}$$

$$\sum_{n=1}^{N} nP_1(n, mL_0)\{-A_{n3}[1 - (-1)^m \cos \overline{\theta}_n^*] + (-1)^m A_{n4} \sin \overline{\theta}_n^*\}$$

$$+ \frac{\pi}{2mL_0{}^2} \left\{ B_{m3} P_2(mL_0)\ \frac{\cos \overline{\varphi}_m^* - \cosh \varphi_m^*}{\sinh \varphi_m{}^*} \right.$$

$$\left. + B_{m4} \left[\frac{P_2(mL_0) \sin \overline{\varphi}_m^*}{\sinh \varphi_m^*} - P_3(mL_0) \right] \right\} = 0 \tag{30}$$

$$\frac{\pi}{2mL_0{}^2} \left\{ A_{m3} \left[P_2(m)\ \frac{\cos \overline{\theta}_m^* \cosh \theta_m^* - 1}{\sinh \theta_m^*} + P_3(m) \sin \overline{\theta}_m^* \right] \right.$$

$$+ A_{m4} \left[P_2(m)\ \frac{\cosh \theta_m^* \sin \overline{\theta}_m^*}{\sinh \theta_m^*} - P_3(m) \cos \overline{\theta}_m^* \right] \right\}$$

$$+ \sum_{n=1}^{N} n(-1)^n P_1(nL_0, m) \left\{ -B_{n3}[1 - (-1)^m \cos \overline{\varphi}_n^*] + (-1)^m B_{n4} \sin \overline{\varphi}_n^* \right\} = 0 \tag{31}$$

$$\frac{\pi}{2mL_0{}^2} \left\{ A_{m3}P_2(m) \frac{\cos \overline{\theta}_m{}^* - \cosh \theta_n{}^*}{\sinh \theta_m{}^*} + A_{m4} \left[P_2(m) \frac{\sin \overline{\theta}_m{}^*}{\sinh \theta_m{}^*} - P_3(m) \right] \right\}$$

$$+ \sum_{n=1}^{N} nP_1(nL_0,m) \left\{ -B_{n3}[1 - (-1)^m \cos \overline{\varphi}_n{}^*] + (-1)^m B_{n4} \sin \overline{\varphi}_n{}^* \right\} = 0 \quad (32)$$

where $\lambda \neq n^2 + m^2 L_0{}^2$ or $\lambda \neq n^2 L_0{}^2 + m^2$ (see appendix B). Each value of m gives a separate equation so the resulting coefficient matrix will be of order 4N. The frequency parameter λ is obtained from the condition that the determinant of the coefficient matrix is zero. One significant difference between these equations and those of the Ritz method is that there is no form of

$$[A] - \lambda^2[B] = 0$$

to these equations since λ is contained in $\theta_m{}^*$, $\overline{\varphi}_m{}^*$, etc. This difference is discussed in the next section.

NUMERICAL COMPUTATIONS METHOD

A discussion of the computation is given not because any new numerical scheme is used (the programs that have been written are made up of existing subroutines) but because each method of solution has certain numerical advantages and disadvantages. For the problem being considered, the Ritz method offers comparatively easy computations with possible low accuracy and, conversely, the series solution offers high accuracy with possible serious numerical difficulties. So, depending on one's needs, either method may be the best to use for a given problem.

Ritz Solution

The form of the Ritz method equation is fairly convenient for computation on a digital computer. For the modes calculated, the matrices were small enough so that no major problems were encountered. The roots were found by the computer varying the frequency over some specified range and detecting when the determinant changed sign. An iteration scheme was then used to converge on the root. The computing was done in single precision. Eventually, if larger matrices are used, a point would be reached where the accuracy had diminished to an unacceptable level but double precision could be used and one might, at least partially, normalize the equations. For instance, the constants a_{0j}, b_{0j}, a_{ij}, b_{ij} could be replaced by $a'_{0j}/j^2 L_0{}^2$, b'_{0j}/j^2, $a'_{ij}/(i^2 + j^2 L_0{}^2)$, $b'_{ij}/(i^2 L_0{}^2 + j^2)$, and the denominators retained in the coefficient matrix.

Series Solution

The equations (29) through (32), as given, can present some serious computational difficulties. One problem is that λ cannot be factored out in the form $[A] - \lambda^2[B] = 0$, so the standard eigenvalue routines cannot be used. The only feasible way of obtaining the frequencies seems to be to plot the determinant as a function of λ and to note the zero values of the determinant. However, as the determinant approaches zero, accuracy is lost and there will be a range of frequency within which the computed determinant has zero-place accuracy and therefore is meaningless. If this range is larger than the range needed to interpolate the frequency to some desired accuracy, the frequency cannot be determined. In the present case, this problem became more prevalent as the plate's length-to-width ratio or matrix size increased. In order to include all of the frequencies listed herein, it was necessary to rearrange equations (29) through (32). Comparing equations (29) and (30) and equations (31) and (32), one sees that the terms inside the summation are identical except for the term $(-1)^n$. By adding or subtracting equations (29) and (30) for each value of m (the same applies to eqs. (31) and (32)), either the odd A_{n3}, A_{n4}'s $(n = 1,3,5,\ldots)$ or the even A_{n3}, A_{n4}'s will vanish. This introduces many more zeros into the matrix and eases the loss-of-accuracy problem. These equations were then normalized by substituting the following for the given constants:

$$\frac{A'_{n3}}{\cosh \frac{\pi m}{L_0}} \; , \qquad \frac{A'_{n4}}{\sinh \frac{\pi m}{L_0}} \; , \qquad \frac{B'_{m3}}{\cosh m\pi} \; , \qquad \frac{B'_{m4}}{\sinh m\pi}$$

One should be careful to normalize with positive nonzero quantities since the quantity, if ever zero, will introduce a point of discontinuity, and possibly a change in sign, into the determinant. When the determinant is plotted, these points may appear to be natural frequencies. The reason for choosing the particular normalizing factors shown is that for large values of m^2, say, $m^2 > 30$, and small values of λ, say, $\lambda < 10$, the large terms in the matrix are of the form

$$\cosh \varphi_m^* = \cosh \pi \sqrt{\lambda + m^2} = O(\cosh m\pi)$$

$$\cos \overline{\theta}_n^* = \cos i \, \pi \sqrt{m^2 - \lambda} = \cosh \pi \sqrt{m^2 - \lambda} = O(\cosh m\pi)$$

so that normalizing these terms by the factor $\cosh m\pi$ makes them about unity. But if higher frequencies are desired such that λ is not small compared to m, this factor may not be adequate and it should be weighted more heavily toward the effect of λ. So, depending on the range of the parameters $(m, L_0, \lambda, \text{etc.})$ being considered, considerable trial-and-error rearrangement of the equations may be necessary.

Finally, double precision was used in the computations and in generating the elements of the matrix. The revised equations are given in appendix C.

EXPERIMENTAL METHODS

A short experimental program was undertaken to see the correlation with the theoretical results. Preliminary testing of a plate that was visibly warped indicated that the frequency was quite sensitive to plate warpage. Therefore, some care was taken to insure that the plates for which the results are presented were flat (a "flat" plate is one in which the maximum deviation is a small percentage of the thickness). The method of support is shown in figures 1 and 2. The supports were adjusted until there was no loss of contact between the support and the plate corner during vibration. This means that some compression was introduced into the plate, but its effect was considered negligible since the force was close to a point load which produced a very small average compressive stress throughout the plate. Changes in the support adjustment gave no measurable difference in natural frequency. Several methods of excitation were used. The primary one for measuring the frequencies was a 30-watt sound speaker that excited the plate through an attached string (see fig. 1). The speaker was driven by a variable frequency oscillator and the motion of the plate was measured by a capacitance-type displacement instrument. Since the string transmitted no net compression, the exciting force was not a complete sine curve but this was considered to have a negligible effect on the measured natural frequency.

Figures 3 and 4 are examples of the often used method of detecting the mode shapes. Sand (carborundum chips were used for the pictures because of their dark color) is sprinkled on the plate during vibration and the particles migrate to the node lines.

RESULTS AND COMPARISON

In the following remarks, the modes are referred to by number (see table I). This can be misleading since the relative magnitude of the frequencies associated with two mode shapes can change as L_0 changes (see modes 6 and 7, table I). But for reference purposes, the modes are numbered in the order in which the frequency occurs over the major portion of the range of L_0 considered.

Table I is the summary of the calculated frequencies along with the corresponding ones of reference 2. The results obtained from the Ritz method were calculated from the mode shapes given in table III, where the largest matrix considered was 12 × 12. The series solution used matrices of order 16, 20, and 24 and all three different sized matrices gave the listed value of frequency for most of the modes and a maximum variation of two digits in the last significant figure for the other modes. The series solution should be considerably more accurate for a given matrix size than the Ritz method because each term of the series satisfies the differential equation of motion, the displacement and moment boundary conditions. The comparison between this solution and reference 2 is seen to be very good. The frequencies in reference 2 were obtained by extrapolating the frequencies found by considering the plate divided into a square gridwork in which the width of the nonsquare

14

plates was divided into 4 and 6 grid spacings and the square plate's width was divided into 5 and 6 spacings. Richardson's h^2 extrapolation formula (ref. 2) was used to obtain the value for an infinite number of mesh points.

There are several interesting points that can be seen from table I. Mode 1 approaches the fundamental frequency of a simply supported beam as L_O increases. The beam frequency is $\lambda = 0.954$ (the beam frequency is adjusted since λ, as defined here, contains Poisson's ratio), and $\lambda = 0.951$ for the plate when $L_O = 2.5$. Modes 2 and 3 for $L_O = 1.0$ have the same frequency but different mode shapes (although, considering symmetry, they are the same). This occurrence is not uncommon in plate problems and at that frequency the mode shape can be either one or some superposition of the two mode shapes. Mode 4 is the same as a flexural mode of an unsupported plate. Ritz treated the case for a square plate and the corresponding frequency parameter is $\lambda = 2.00$ (Ritz's calculations, reported in ref. 5, were for $\nu = 0.225$, so the value was scaled up to $\nu = 0.3$ by use of ref. 2). It is interesting to note how this mode shape changes for a nonsquare plate (see table I and fig. 3). In figure 3, it appears as if the node line does not intersect the support point but theoretical results show that is passes very close to the edge of the plate in the region of the corner. Later tests showed this discrepancy was caused by some slight support motion due to the vibration of the test fixture which apparently had a natural frequency near the exciting frequency.

It is also of interest to see the number of other problems solved. Looking at the mode shapes in table I, all of the straight node lines are lines of antisymmetry along which the bending moment is zero. These, then, correspond to simply supported boundaries and can be considered to be plate edges. So, for example, modes 2, 5, and 6 give the first, second, and third mode of a plate simply supported along one edge and point supported at the other two corners (for the range of L_O given and substituting, of course, the proper length and width of the plate). Mode 4, for $L_O = 1.0$, gives the fundamental mode of a 45° right triangular plate simply supported along two edges, or the second mode of a 45° right triangular plate supported along the hypotenuse and at the opposite corner.

After the results were compared, the Ritz method was extended for modes 1, 4, and 7 for $L_O = 1.0$ to see how slow the convergence was. This result is shown in figure 5. Mode 4 is seen to converge very fast. For just two terms, which are

$$w = a_{01} \left(\sin \frac{\pi y}{b} - \sin \frac{\pi x}{a} \right)$$

the answer is within 1 percent. However, mode 7 has an error of about 4 percent after 32 terms. For modes 1 and 7, the results for matrices of order 2, 8, 10, and 12 suggest that the series has converged (see dashed lines in fig. 5) when, actually, convergence has not been reached even with a matrix of order 32. This shows that even though one knows an approximate frequency is an upperbound, it is hard to tell the accuracy of an answer without comparison with a known solution.

Table II shows the comparison between experiment and theory (the series solution and ref. 2) and the correlation is very good. No attempt will be made to explain the small differences because the experiment was of a careful, but not precise, nature.

CONCLUSIONS

One important conclusion common to many plate problems is that one has to be very careful in tracing the modes as the plate changes its dimensions (i.e., from a square to a rectangle). The relative order of frequency can change as can the mode shapes. The fact that mode shapes can change is especially important when one is concerned about the location of nodal and antinodal regions.

The Ritz method yields equations which are easily adapted to the computer but the convergence is hard to predict. The fact that the frequency is about the same for different numbers of terms hopefully means that the assumed displacement has converged to the correct answer, but it may mean that the assumed displacement is converging very slowly and many more terms are needed. Of course, one would expect a higher accuracy for a given number of terms if a displacement function that satisfied at least some of the stress boundary conditions could have been chosen.

The series solution presents some serious computational difficulties for certain ranges of the parameters but for this particular problem one has more confidence in its accuracy for a given matrix size since all of the boundary conditions are satisfied except the effective shear condition by each term in the series.

Ames Research Center
    National Aeronautics and Space Administration
        Moffett Field, Calif., June 28, 1965

APPENDIX A

UNCOUPLED EQUATIONS OF THE RITZ METHOD

It was pointed out in the text that the sets of equations for determining the frequencies by the Ritz method uncouple into four groups of equations. The equations of each group represent modes with certain symmetry characteristics, so if a certain class of modes is desired, considerable simplification is obtained if the appropriate group of equations is used. Using the notation:

$$R_1(i,j,m) = n^2 L_0^2 (i^2 L_0^2 + \nu j^2)$$

$$R_2(i,j,n) = n^2 (i^2 + \nu j^2 L_0^2)$$

$$R_3(j,m,n) = j^2 L_0^2 (m^2 L_0^2 + \nu n^2)$$

$$R_4(j,m,n) = j^2 (m^2 + \nu n^2 L_0^2)$$

$$R_5(i,j,m,n) = n^2 i^2 + m^2 j^2 L_0^4 + (2-\nu) m^2 i^2 L_0^2 + \nu n^2 j^2 L_0^2$$

$$R_6(i,j,m,n) = n^2 i^2 L_0^4 + m^2 j^2 + (2-\nu) m^2 i^2 L_0^2 + \nu n^2 j^2 L_0^2$$

the equations are:

Combination (1)

$$a_{oj} 2(j^4 L_0^4 - \lambda^2) + \frac{16}{\pi^2 j} \sum_{n=1,3,\ldots} \frac{b_{on}(\nu n^2 j^2 L_0^2 - \lambda^2)}{n}$$

$$+ \frac{16j}{\pi^2} \sum_{\substack{m=2,4,\ldots \\ n=1,3,\ldots}} \frac{b_{mn}[R_1(j,m,n) - \lambda^2]}{n(j^2 - m^2)} = 0 \qquad (A1)$$

$$b_{oj} 2(j^4 - \lambda^2) + \frac{16}{\pi^2 j} \sum_{n=1,3,\ldots} \frac{a_{on}(\nu n^2 j^2 L_0^2 - \lambda^2)}{n}$$

$$+ \frac{16j}{\pi^2} \sum_{\substack{m=2,4,\ldots \\ n=1,3,\ldots}} \frac{a_{mn}[R_2(j,m,n) - \lambda^2]}{n(j^2 - m^2)} = 0 \qquad (A2)$$

17

$$a_{ij}[(i^2+j^2L_o^2)^2-\lambda^2] + \frac{16}{\pi^2 j} \sum_{n=1,3,\ldots} \frac{b_{on}n[R_2(i,j,n)-\lambda^2]}{n^2-i^2}$$

$$+ \frac{16j}{\pi^2} \sum_{\substack{m=2,4,\ldots \\ n=1,3,\ldots}} \frac{b_{mn}n[R_5(i,j,m,n)-\lambda^2]}{(n^2-i^2)(j^2-m^2)} = 0 \qquad (A3)$$

$$b_{ij}[(i^2L_o^2+j^2)^2-\lambda^2] + \frac{16}{\pi^2 j} \sum_{n=1,3,\ldots} \frac{a_{on}n[R_1(i,j,m)-\lambda^2]}{n^2-i^2}$$

$$+ \frac{16j}{\pi^2} \sum_{\substack{m=2,4,\ldots \\ n=1,3,\ldots}} \frac{a_{mn}n[R_6(i,j,m,n)-\lambda^2]}{(n^2-i^2)(j^2-m^2)} = 0 \qquad (A4)$$

Combination (2)

$$b_{oj}2(j^4-\lambda^2) + \frac{16j}{\pi^2} \sum_{\substack{m=1,3,\ldots \\ n=1,3,\ldots}} \frac{a_{mn}[R_4(j,m,n)-\lambda^2]}{n(j^2-m^2)} = 0 \qquad (A5)$$

$$a_{ij}[(i^2+j^2L_o^2)^2-\lambda^2] + \frac{16}{\pi^2 j} \sum_{n=2,4,\ldots} \frac{b_{on}n[R_2(i,j,n)-\lambda^2]}{n^2-i^2}$$

$$+ \frac{16j}{\pi^2} \sum_{\substack{m=2,4,\ldots \\ n=2,4,\ldots}} \frac{b_{mn}n[R_5(i,j,m,n)-\lambda^2]}{(n^2-i^2)(j^2-m^2)} = 0 \qquad (A6)$$

$$b_{ij}[(i^2L_o^2+j^2)^2-\lambda^2] + \frac{16j}{\pi^2} \sum_{\substack{m=1,3,\ldots \\ n=1,3,\ldots}} \frac{a_{mn}n[R_6(i,j,m,n)-\lambda^2]}{(n^2-i^2)(j^2-m^2)} = 0 \qquad (A7)$$

Combination (3)

$$a_{oj}2(j^4L_o^4-\lambda^2) + \frac{16j}{\pi^2} \sum_{\substack{m=1,3,\ldots \\ n=1,3,\ldots}} \frac{b_{mn}[R_3(j,m,n)-\lambda^2]}{n(j^2-m^2)} = 0 \qquad (A8)$$

$$a_{ij}[(i^2+j^2L_o^2)^2-\lambda^2] + \frac{16j}{\pi^2} \sum_{\substack{m=1,3,\ldots \\ n=1,3,\ldots}} \frac{b_{mn}n[R_5(i,j,m,n)-\lambda^2]}{(n^2-i^2)(j^2-m^2)} = 0 \qquad (A9)$$

$$b_{ij}[(i^2L_o^2+j^2)^2-\lambda^2] + \frac{16}{\pi^2 j} \sum_{n=2,4,\ldots} \frac{a_{on}n[R_1(i,j,m)-\lambda^2]}{n^2-i^2}$$

$$+ \frac{16j}{\pi^2} \sum_{\substack{m=2,4,\ldots \\ n=2,4,\ldots}} \frac{a_{mn}n[R_6(i,j,m,n)-\lambda^2]}{(n^2-i^2)(j^2-m^2)} = 0 \qquad (A10)$$

Combination (4)

$$a_{ij}[(i^2+j^2L_o^2)^2-\lambda^2] + \frac{16j}{\pi^2} \sum_{\substack{m=1,3,\ldots \\ n=2,4,\ldots}} \frac{b_{mn}n[R_5(i,j,m,n)-\lambda^2]}{(n^2-i^2)(j^2-m^2)} = 0 \qquad (A11)$$

$$b_{ij}[(i^2L_o^2+j^2)^2-\lambda^2] + \frac{16j}{\pi^2} \sum_{\substack{m=1,3,\ldots \\ n=2,4,\ldots}} \frac{a_{mn}n[R_6(i,j,m,n)-\lambda^2]}{(n^2-i^2)(j^2-m^2)} = 0 \qquad (A12)$$

DISCUSSION OF ASSUMPTION IN THE DERIVATION OF EQUATION (14)

In the derivation of the solution to equation (14), it was assumed that $f_n(y) \sin \alpha_n x$ was independent of $g_n(x) \sin \beta_n y$ and later, in integrating the equations for the shear boundary condition, it was assumed that $\overline{\theta}_n \neq m$ which is the same as assuming $\lambda \neq n^2 + m^2 L_0{}^2$. When the frequencies are found by plotting the determinant versus λ, the points $\lambda = n^2 + m^2 L_0{}^2$ cannot be calculated from the equations in their given form since some terms become indeterminant. But, assuming the determinant is a continuous function of λ, it appears as if it is identically zero for all the matrix sizes considered for $\lambda = n^2 + m^2 L_0{}^2$. One recognizes that these frequencies are identical to those of a plate that is simply supported on all edges. If

$$f_n(y) \sin \alpha_n x = g_m(x) \sin \beta_m y = a_{mn} \sin \beta_m y \sin \alpha_n x$$

the displacement is

$$w = a_{mn} \sin \beta_m y \sin \alpha_n x$$

and is a solution to the equation of motion if

$$\lambda = n^2 + m^2 L_0{}^2$$

But, in order to satisfy the shear boundary conditions, the following type of equations must hold:

$$a_{mn} \alpha_n [\alpha_n{}^2 - (2-\nu)\beta_m{}^2] \sin \beta_m y = 0$$

$$a_{mn} \beta_m [\beta_m{}^2 - (2-\nu)\alpha_n{}^2] \sin \alpha_n x = 0$$

These equations are for zero shear at $x = 0$ and $y = 0$. It is seen that $a_{mn} = 0$. Therefore, the plate cannot have the same frequency and mode shape as a simply supported plate, that is, it cannot have zero displacement and zero shear along the same edge without having zero displacement everywhere. The remaining question is whether the plate can have the same frequency but a different mode shape. An example of this is that a beam with built-in ends has the same frequencies but different mode shapes as a beam with free ends. This question does not appear to have an obvious answer, in general, but the equations were modified to allow λ to have a value of, say, $\overline{n}^2 + \overline{m}^2 L_0{}^2$, and it was apparent that considerable uncoupling occurs. (For instance, $\sin \overline{\theta}_{\overline{n}}{}^* = \sin \overline{\varphi}_{\overline{m}}{}^* = 0$; $1 - (-1)^{\overline{m}} \cos \overline{\theta}_{\overline{n}}{}^* = 0$.) It is easily seen in the small matrices how the constants A_{n3}, A_{n4}, B_{n3}, B_{n4} all have to be zero. A 4×4 and an 8×8 matrix were investigated and the equations uncoupled in such a way that all constants had to be zero so there was no motion at that

frequency. These frequencies are not present either in the Ritz solution or in the experimental work so it is concluded that even though they represent roots of the determinant, they do not represent a mode that has motion.

MODIFIED EQUATIONS FOR THE SERIES SOLUTIONS

The modified equations which avoid numerical problems encountered for some of the modes are given by

$$\sum_{\substack{n=2,4,\ldots \\ n=1,3,\ldots}} \pm 2nP_1(n,mL_0) \left\{ \frac{-A'_{n3}[1-(-1)^m \cos \overline{\theta}_n{}^*]}{\cosh \frac{\pi m}{L_0}} + \frac{(-1)^m A'_{n4} \sin \overline{\theta}_n{}^*}{\sinh \frac{\pi m}{L_0}} \right\}$$

$$+ \frac{\pi}{2mL_0{}^2} \left\{ B'_{m3} \left[\frac{P_2(mL_0)(\cosh \varphi_m{}^* \pm 1)(\cos \overline{\varphi}_m{}^* \mp 1)}{\sinh \varphi_m{}^* \cosh m\pi} + \frac{P_3(mL_0)\sin \overline{\varphi}_m{}^*}{\cosh m\pi} \right] \right.$$

$$\left. + B'_{m4} \left[\frac{P_2(mL_0)\sin \overline{\varphi}_m{}^*(\cosh \varphi_m{}^* \pm 1)}{\sinh \varphi_m{}^* \sinh m\pi} - \frac{P_3(mL_0)(\cos \overline{\varphi}_m{}^* \pm 1)}{\sinh m\pi} \right] \right\} = 0 \quad (C1,2)$$

$$\frac{\pi}{2mL_0} \left\{ A'_{m3} \left[\frac{P_2(m)(\cosh \theta_m{}^* \pm 1)(\cos \overline{\theta}_m{}^* \mp 1)}{\sinh \theta_m{}^* \cosh \frac{\pi m}{L_0}} + \frac{P_3(m)\sin \overline{\theta}_m{}^*}{\cosh \frac{\pi m}{L_0}} \right] \right.$$

$$\left. + A'_{m4} \left[\frac{P_2(m)\sin \overline{\theta}_m{}^*(\cosh \theta_m{}^* \pm 1)}{\sinh \theta_m{}^* \sinh \frac{\pi m}{L_0}} - \frac{P_3(m)(\cos \overline{\theta}_m{}^* \pm 1)}{\sinh \frac{\pi m}{L_0}} \right] \right\}$$

$$+ \sum_{\substack{n=2,4,\ldots \\ n=1,3,\ldots}} \pm 2nP_1(nL_0,m) \left\{ \frac{-B'_{n3}[1-(-1)^m \cos \overline{\varphi}_n{}^*]}{\cosh n\pi} + \frac{(-1)^m B'_{n4} \sin \overline{\varphi}_n{}^*}{\sinh n\pi} \right\} = 0 \quad (C3,4)$$

where for

equations (C1,3)   n = 2,4,6,. . .   m = 1,2,3,4,. . .

$\pm$ use +, $\mp$ use -

equations (C2,4)   n = 1,3,5,. . .   m = 1,2,3,4,. . .

$\pm$ use -, $\mp$ use +

REFERENCES

1. Harris, Cyril M.; and Crede, Charles E.: Shock and Vibration Handbook. Vol. 1, McGraw-Hill Book Co., Inc., New York, 1961.

2. Cox, Hugh L.; and Boxer, Jack: Vibration of Rectangular Plates Point-Supported at the Corners. The Aero. Quart., vol. XI, Part 1, London, Feb. 1960, p. 41-50.

3. Timoshenko, Stephen; and Woinowsky-Krieger, S.: Theory of Plates and Shells. Second ed., McGraw-Hill Book Co., Inc., New York, 1959, p. 85.

4. Young, Dana: Vibration of Rectangular Plates by the Ritz Method. ASME Trans. (J. Appl. Mech.), vol. 17, no. 4, Dec. 4, 1950, p. 448-453.

5. Timoshenko, Stephen, ed.; and Young, D. H.: Vibration Problems in Engineering. Third ed., D. Van Nostrand Co., Inc., New York, 1955, p. 445.

TABLE I.- SUMMARY OF CALCULATED FIGURES

$$\lambda = \omega \, \frac{a^2}{\pi^2} \sqrt{\frac{\gamma h}{Dg}} \;\; ; \;\; \nu = 0.3$$

Mode	L_o	Ref. 2	Ritz solution	Series solution
1. (diagram: +)	1.0	0.721	0.756	0.721
	1.5	.904	.933	.904
	2.0	.938	.958	.941
	2.5	---	.961	.951
2. (diagram: + / −)	1.0	1.594	1.702	1.598
	1.5	---	2.308	2.181
	2.0	---	2.941	2.786
3. (diagram: + | −)	1.0	1.594	1.702	1.598
	1.5	---	2.811	2.616
	2.0	---	3.52	3.326
4. (diagram)	1.0	1.938	1.986	1.986
	1.5	---	3.53	3.414
	2.0	---	5.69	5.27
5. (diagram: + − / − +)	1.0	3.896	4.20	3.895
	1.5	---	5.67	5.34
	2.0	---	6.80	6.46
6. (diagram: + − + −)	1.0	---	5.23	5.10
	1.5	---	5.85	5.85
	2.0	---	7.40	7.22
7. (diagram: + / ⊖)	1.0	4.411	4.89	4.50
	1.5	---	7.64	7.10

24

TABLE II.- COMPARISON OF EXPERIMENT AND THEORY

| Mode	Plate 1 12 × 12 × 0.129 inch 2024 aluminum $E = 10.6 \times 10^6$, psi (book value)			Plate 2 10 × 20 × 0.173 inch 2024 aluminum $E = 10.6 \times 10^6$, psi (book value)		
	Ref. 2	Experiment	Series solution	Ref. 2	Experiment	Series solution
1.	61.4 cps	62 cps	61.4 cps	38.8 cps	38.3 cps	38.8 cps
2.	136	134	136	---	113	115
3.	136	134	136	---	136	137
4.	166	169	170	---	214	218
5.	333	330	333	---	261	267
6.	---	434	436	---	294	298
7.	375	383	385	---	---	---

TABLE III.- RITZ METHOD MODE SHAPES

Mode 1 | + |

Mode 2 | + | − |

a/b	Frequency parameter, λ	Normalized mode-shape coefficients		Frequency parameter, λ	Normalized mode-shape coefficients	
1.0	0.756	$a_{01} = 1.000$ $a_{03} = -.0663$ $a_{21} = .1737$ $a_{23} = .0329$ $a_{41} = -.0267$	$b_{01} = 1.000$ $b_{03} = -.0663$ $b_{21} = .1737$ $b_{23} = .0329$ $b_{41} = -.0267$	1.702	$a_{02} = -0.1248$ $a_{04} = -.0075$ $a_{22} = .1695$ $a_{24} = -.0055$ $a_{42} = -.0146$	$b_{11} = 1.000$ $b_{13} = -.0671$ $b_{31} = -.0574$ $b_{33} = .0348$ $b_{51} = -.0083$
1.5	.933	$a_{01} = .0869$ $a_{03} = -.0150$ $a_{21} = .0950$ $a_{23} = .0056$ $a_{41} = -.0102$	$b_{01} = 1.000$ $b_{03} = -.0320$ $b_{21} = .0281$ $b_{23} = .0161$ $b_{41} = -.0068$	2.308	$a_{02} = -.1753$ $a_{04} = .0002$ $a_{22} = .1530$ $a_{24} = -.0059$ $a_{42} = .0012$ $a_{06} = .0009$	$b_{11} = 1.000$ $b_{13} = -.0499$ $b_{31} = -.0748$ $b_{33} = .0205$ $b_{51} = -.0062$ $b_{15} = -.0065$
2.0	.958	$a_{01} = -.0054$ $a_{03} = -.0052$ $a_{21} = .570$ $a_{23} = .0013$ $a_{41} = -.0035$	$b_{01} = 1.000$ $b_{03} = -.0179$ $b_{21} = .0046$ $b_{23} = .0080$ $b_{41} = -.0025$	2.941	$a_{02} = -.1915$ $a_{04} = .0067$ $a_{22} = .1537$ $a_{24} = -.0088$ $a_{42} = .0080$ $a_{06} = .0007$	$b_{11} = 1.000$ $b_{13} = -.0460$ $b_{31} = -.0893$ $b_{33} = .0159$ $b_{51} = -.0028$ $b_{15} = -.0093$
2.5	.961	$a_{01} = -.0197$ $a_{03} = -.0020$ $a_{21} = .0372$ $a_{23} = .0002$ $a_{41} = -.0007$	$b_{01} = 1.000$ $b_{03} = -.0108$ $b_{21} = -.0014$ $b_{23} = .0042$ $b_{41} = -.0011$	3.60	$a_{02} = -.1984$ $a_{04} = .0100$ $a_{22} = .1550$ $a_{24} = -.0103$ $a_{42} = .0120$ $a_{06} = .0005$	$b_{11} = 1.000$ $b_{13} = -.0451$ $b_{31} = -.0967$ $b_{33} = .0135$ $b_{51} = -.0009$ $b_{15} = -.0113$

TABLE III.- RITZ METHOD MODE SHAPES - Continued

Mode 3 [+|−] Mode 4 [⊠ with +/−/−/+]

a/b	Frequency parameter, λ	Normalized mode-shape coefficients		Frequency parameter, λ	Normalized mode-shape coefficients	
1.0	1.702	$a_{11} = 1.000$ $a_{13} = -.0671$ $a_{31} = -.0574$ $a_{33} = .0348$ $a_{51} = -.0083$	$b_{02} = -0.1248$ $b_{04} = -.0075$ $b_{22} = .1695$ $b_{24} = -.0055$ $b_{42} = -.0146$	1.986	$a_{01} = 1.000$ $a_{03} = -.0244$ $a_{21} = -.0802$ $a_{23} = .0112$ $a_{41} = .0049$	$b_{01} = -1.000$ $b_{03} = .0244$ $b_{21} = .0802$ $b_{23} = -.0112$ $b_{41} = -.0049$
1.5	2.811	$a_{11} = 1.000$ $a_{13} = -.0817$ $a_{31} = .0205$ $a_{33} = .0428$ $a_{51} = -.0209$	$b_{02} = .1539$ $b_{04} = -.0380$ $b_{22} = .1850$ $b_{24} = .0115$ $b_{42} = -.0230$	3.53	$a_{01} = 1.000$ $a_{03} = -.0536$ $a_{21} = .0756$ $a_{23} = .0255$ $a_{41} = -.0107$	$b_{01} = -.8108$ $b_{03} = .0002$ $b_{21} = .1693$ $b_{23} = .0171$ $b_{41} = -.0191$
2.0	3.52	$a_{11} = .7924$ $a_{13} = -.0877$ $a_{31} = .1496$ $a_{33} = .0426$ $a_{51} = -.0304$	$b_{02} = 1.000$ $b_{04} = -.0808$ $b_{22} = .1713$ $b_{24} = .0334$ $b_{42} = -.0272$	5.69	$a_{01} = 1.000$ $a_{03} = -.0726$ $a_{21} = .2048$ $a_{23} = .0322$ $a_{41} = .0011$	$b_{01} = -.742$ $b_{03} = .0903$ $b_{21} = .2277$ $b_{23} = .0341$ $b_{41} = -.0277$
2.5	3.77	$a_{11} = .1928$ $a_{13} = -.0337$ $a_{31} = .1130$ $a_{33} = .0150$ $a_{51} = -.0109$	$b_{02} = 1.000$ $b_{04} = -.0479$ $b_{22} = .0536$ $b_{24} = .0191$ $b_{42} = -.0112$	10.30	$a_{01} = .8438$ $a_{03} = -.3091$ $a_{21} = -.8536$ $a_{23} = .2419$ $a_{41} = .0530$	$b_{01} = -.8072$ $b_{03} = .1068$ $b_{21} = 1.000$ $b_{23} = -.1570$ $b_{41} = -.1440$

TABLE III.- RITZ METHOD MODE SHAPES - Continued

Mode 5 | Mode 6

a/b	Frequency parameter, λ	Normalized mode-shape coefficients		Frequency parameter, λ	Normalized mode-shape coefficients	
1.0	4.20	$a_{12} = 1.000$ $a_{14} = -.1458$ $a_{32} = .2107$ $a_{34} = .0645$ $a_{52} = -.0433$ $a_{16} = -.0053$	$b_{12} = 1.000$ $b_{14} = -.1458$ $b_{32} = .2107$ $b_{34} = .0645$ $b_{52} = -.0433$ $b_{16} = -.0053$	5.23	$a_{11} = 1.000$ $a_{13} = -.0629$ $a_{31} = -.2789$ $a_{33} = -.0007$ $a_{51} = .0318$	$b_{02} = -0.9796$ $b_{04} = .0944$ $b_{22} = .0337$ $b_{24} = -.0492$ $b_{42} = -.0000$
1.5	5.67	$a_{12} = -.0666$ $a_{14} = -.0342$ $a_{32} = .1809$ $a_{34} = .0119$ $a_{52} = -.0049$ $a_{16} = .0014$	$b_{12} = 1.000$ $b_{14} = -.0797$ $b_{32} = -.0153$ $b_{34} = .0326$ $b_{52} = -.0190$ $b_{16} = -.0101$	5.85	$a_{11} = 1.000$ $a_{13} = -.0446$ $a_{31} = -.1487$ $a_{33} = .0225$ $a_{51} = .0084$	$b_{02} = -.8072$ $b_{04} = .0477$ $b_{22} = .1222$ $b_{24} = -.0232$ $b_{42} = -.0078$
2.0	6.80	$a_{12} = -.1869$ $a_{14} = -.0122$ $a_{32} = .1764$ $a_{34} = .0011$ $a_{52} = .0068$ $a_{16} = .0015$	$b_{12} = 1.000$ $b_{14} = -.0671$ $b_{32} = -.0548$ $b_{34} = .0238$ $b_{52} = -.0114$ $b_{16} = -.0134$	7.40	$a_{11} = 1.000$ $a_{13} = -.0597$ $a_{31} = -.0626$ $a_{33} = .0316$ $a_{51} = -.0013$	$b_{02} = -.6479$ $b_{04} = .0324$ $b_{22} = .1557$ $b_{24} = -.0051$ $b_{42} = -.0151$
2.5	7.95	$a_{12} = -.2238$ $a_{14} = -.0021$ $a_{32} = .1772$ $a_{34} = -.0038$ $a_{52} = .0134$ $a_{16} = .0013$	$b_{12} = 1.000$ $b_{14} = -.0630$ $b_{32} = -.0717$ $b_{34} = .0195$ $b_{52} = -.0074$ $b_{16} = -.0160$	9.88	$a_{11} = 1.000$ $a_{13} = -.0705$ $a_{31} = -.0104$ $a_{33} = .0364$ $a_{51} = .0059$	$b_{02} = -.5687$ $b_{04} = .0720$ $b_{22} = .1772$ $b_{24} = .0027$ $b_{42} = -.0195$

TABLE III.- RITZ METHOD MODE SHAPES - Concluded

Mode 7

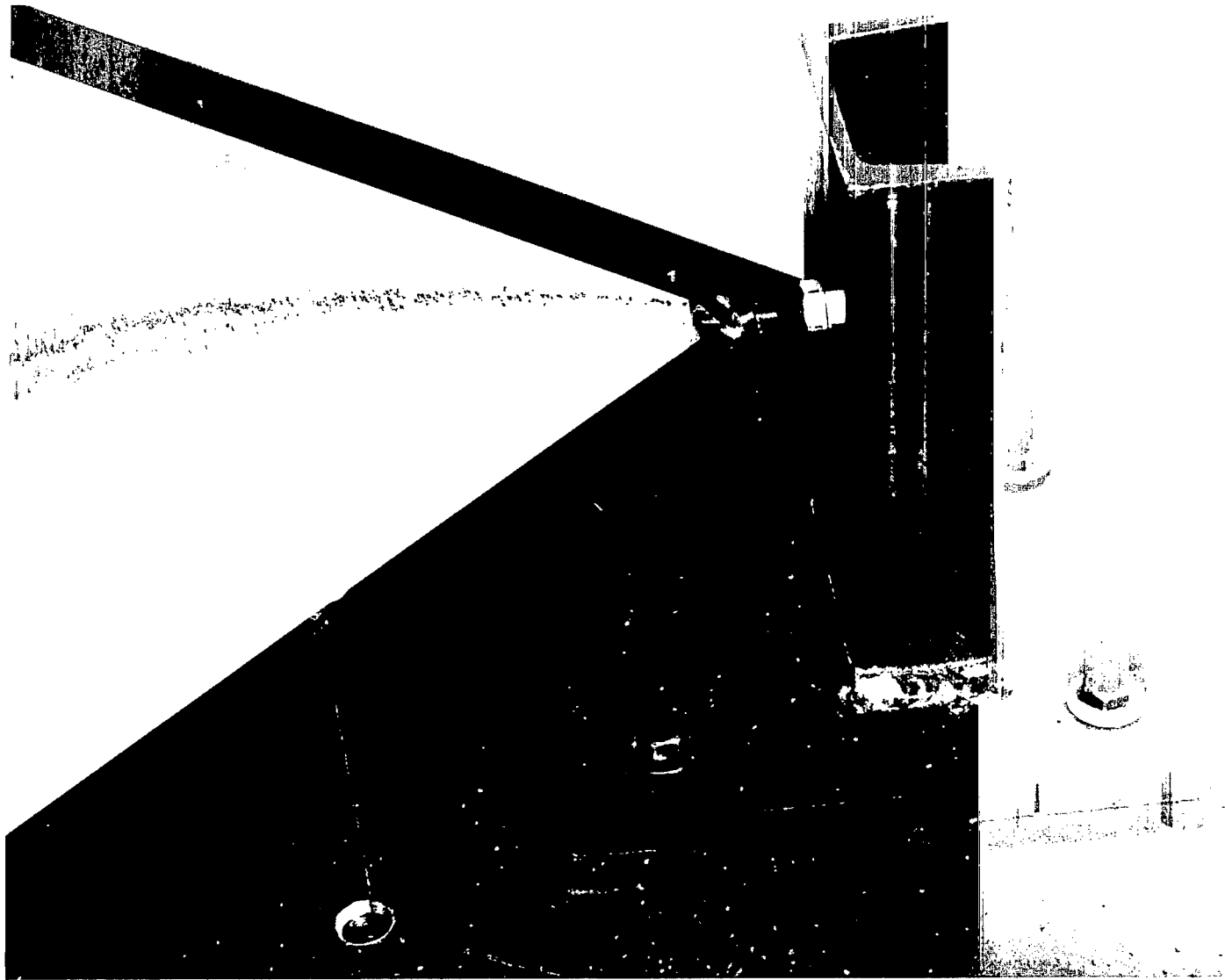| a/b	Frequency parameter, λ	Normalized mode-shape coefficients	
1.0	4.89	$a_{01} = 0.1555$ $a_{03} = -.1950$ $a_{21} = 1.000$ $a_{23} = .1088$ $a_{41} = -.0988$	$b_{01} = 0.1555$ $b_{03} = -.1950$ $b_{21} = 1.000$ $b_{23} = .1088$ $b_{41} = -.0988$
1.5	7.64	$a_{01} = -.4491$ $a_{03} = -.1209$ $a_{21} = 1.000$ $a_{23} = .0468$ $a_{41} = -.0658$	$b_{01} = .6498$ $b_{03} = -.0355$ $b_{21} = .5491$ $b_{23} = .1078$ $b_{41} = -.0590$

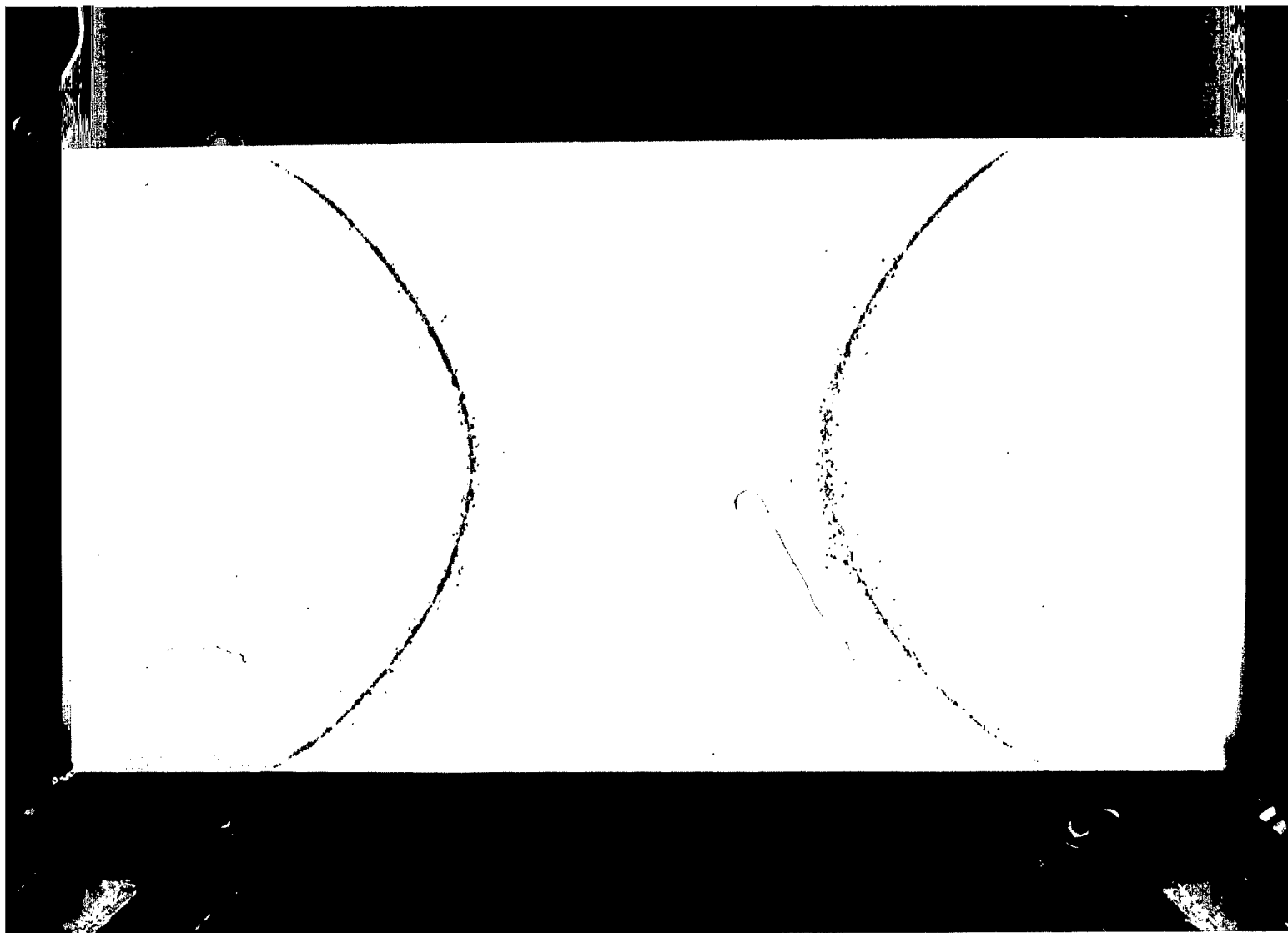Figure 1.- Method of support and excitation.
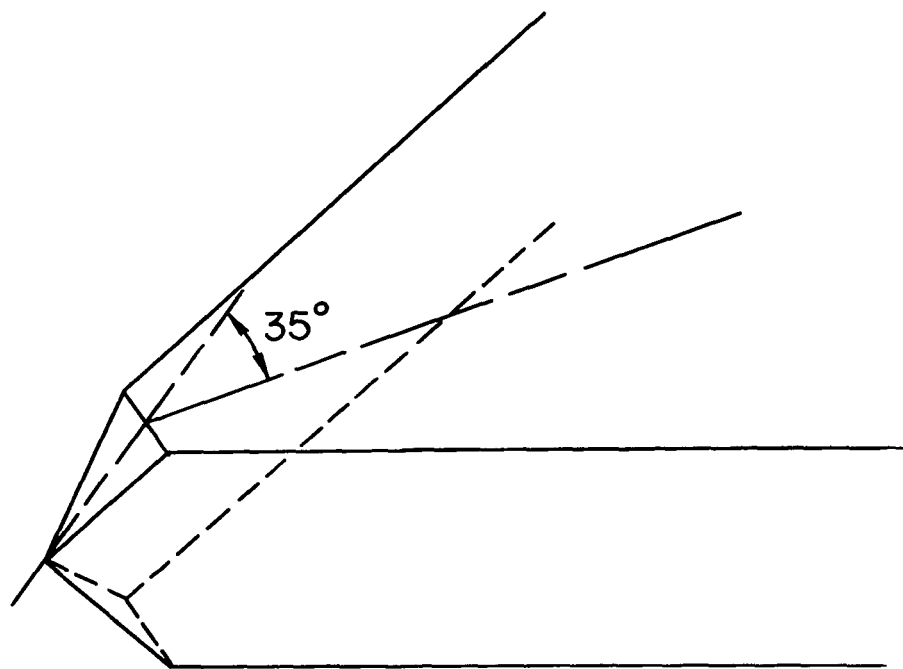
Figure 2.- Detail of plate corner.

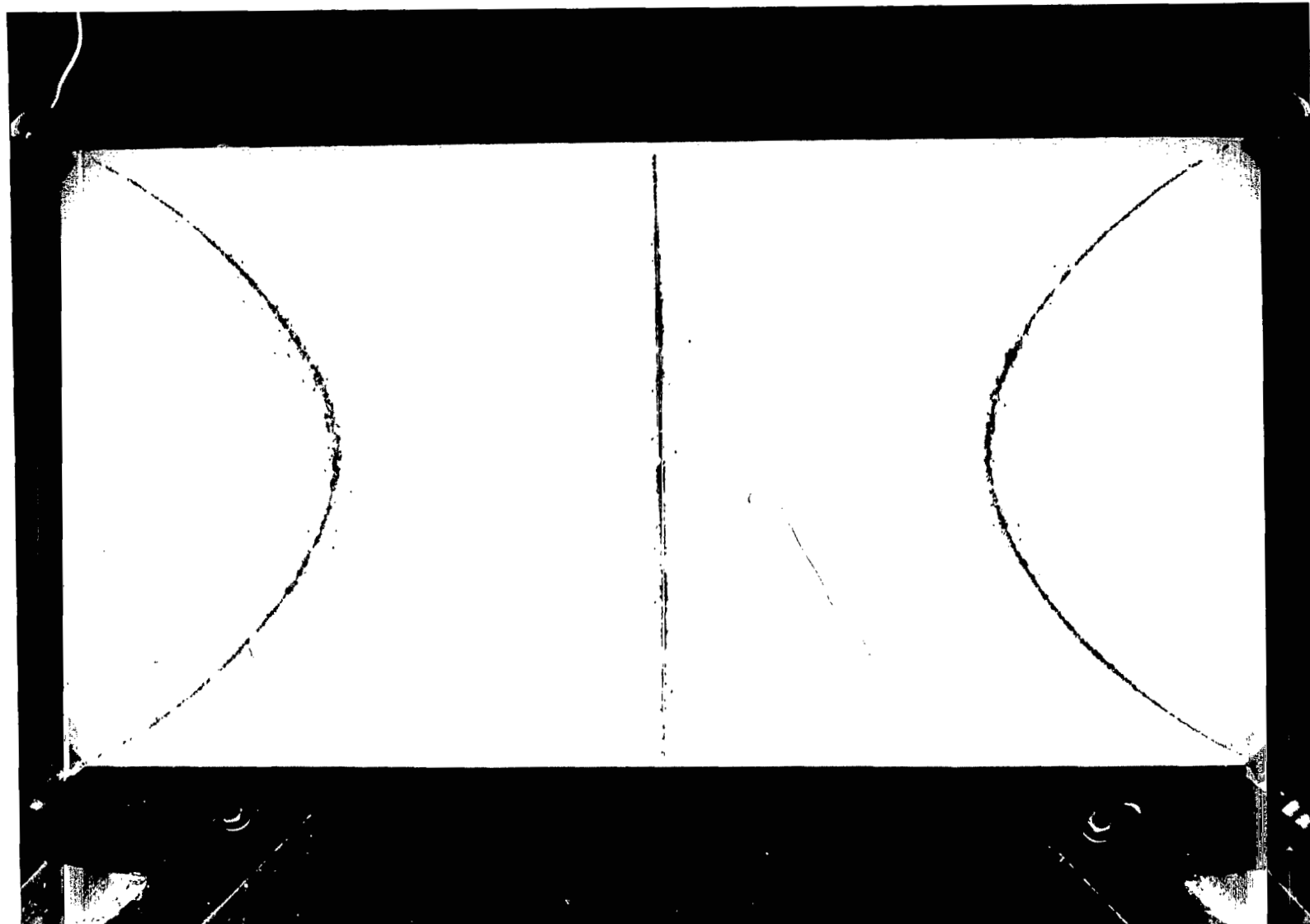Figure 3.- Experimentally determined shape of mode 4.
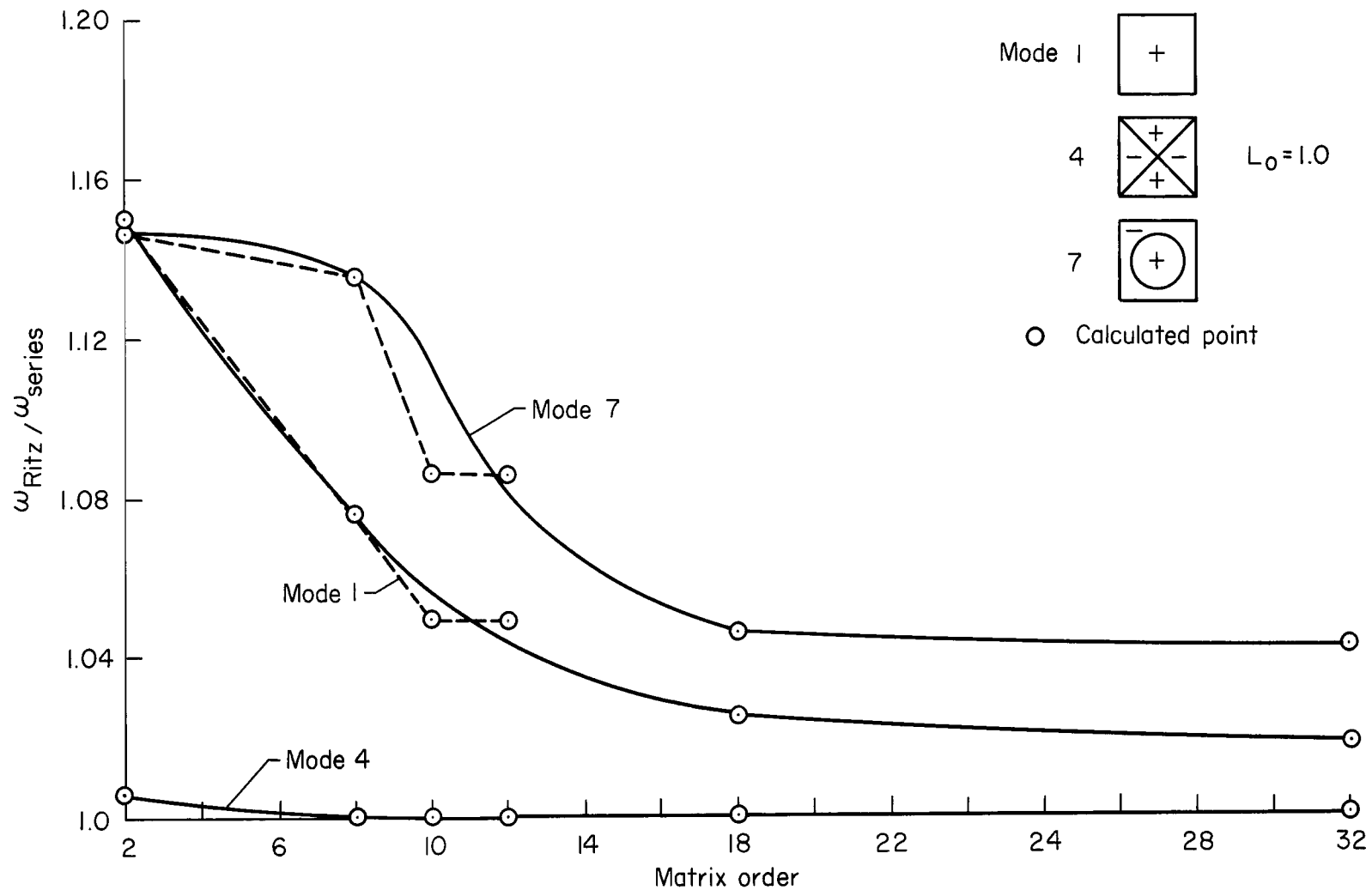
Figure 4.- Experimentally determined shape of mode 6.

A-33922

Figure 5.- Examples of Ritz method convergence.